Intracranial meningioma.

L A Sheporaitis, A G Osborn, J G Smirniotopoulos, D A Clunie, J Howieson and A N D'Agostino

AJNR Am J Neuroradiol 1992, 13 (1) 29-37
http://www.ajnr.org/content/13/1/29

Radiologic-Pathologic Correlation

Intracranial Meningioma

Lori A. Sheporaitis,[1] *Anne G. Osborn, James G. Smirniotopoulos, David A. Clunie, John Howieson, and A. N. D'Agostino*

From the University of Vermont College of Medicine, Burlington, VT (LAS); University of Utah School of Medicine, Salt Lake City, UT (AGO); Armed Forces Institute of Pathology, Washington, DC (JGS, AGO); Oregon Health Sciences University, Portland, OR (DAC, JH, AND); and Uniformed Services University of the Health Sciences, Bethesda, MD (JGS)

Clinical History

A 56-year-old woman experienced progressive dementia for several years. She had no focal neurologic findings. As part of an evaluation for Alzheimer disease a computed tomography (CT) scan of the head was obtained (Fig. 1), following which magnetic resonance imaging (MR) was performed (Figs. 2A-2D).

Additional MR scans are shown (Figs. 2E-2I). The patient died from a probable myocardial infarction before surgery could be performed. Coronal brain sections (Fig. 3) from a post-mortem examination limited to the head disclosed meningioma. Histologic features of a transitional-type meningioma were present (Fig. 4).

Discussion: Intracranial Meningioma

General

Meningioma is the most common primary nonglial intracranial neoplasm, representing 15%–20% of all primary brain tumors. It has a peak incidence in the fifth and sixth decades, with a 2:1 preponderance in females (1). It is generally benign and surgically treatable, with a local recurrence rate of 20 to 30% (2) (Footnote A).

Location

Meningiomas are thought to arise from arachnoid cap cells and are most commonly located at sites of arachnoid granulations along the dura, particularly near venous sinuses. Ten to fifteen percent originate in the posterior fossa or spinal canal. Approximately 90% are supratentorial. Twenty-five percent are parasagittal, 20% arise along the convexity, and 40% are anterior basal (including sphenoid ridge, olfactory groove, and diaphragma sellae). Less common intracranial locations include the cerebellopontine angle, clivus, foramen magnum, cerebral ventricles, and pineal region (3).

Sphenoid ridge meningiomas may be either rounded or flat and extend into the anterior or middle cranial fossa (3). The tumor in this case is large and globular, arising from the sphenoid ridge (Figs. 1A, 2E, and 2H) and extending into both the anterior and middle cranial fossae (Figs. 1C and 2A-2F). Sphenoid meningiomas with medial extension may also involve the optic nerve, encase the supraclinoid carotid artery (Fig. 2G), and invade the cavernous sinus (Footnote A). Sphenoid ridge meningiomas arising more laterally (pterional) often present en plaque, can demonstrate extensive hyperostosis, and may invade through the bone into the overlying temporalis muscle (Footnote A).

Footnote A: Naidich TP. Imaging Evaluation of Meningiomas. In: *Neoplasms of the CNS*, an ASNR categorical course syllabus. Course presented in Los Angeles, CA, March 19–23, 1990.

[1] Address reprint requests to Anne G. Osborn, Department of Radiology, University of Utah Medical Center, 50 North Medical Drive, Salt Lake City, UT 84132.

Index terms: Radiologic-pathologic correlations; Meninges, neoplasms; Brain neoplasms; Neuropathology

AJNR 13:29–37, Jan/Feb 1992 0195-6108/92/1301-0029

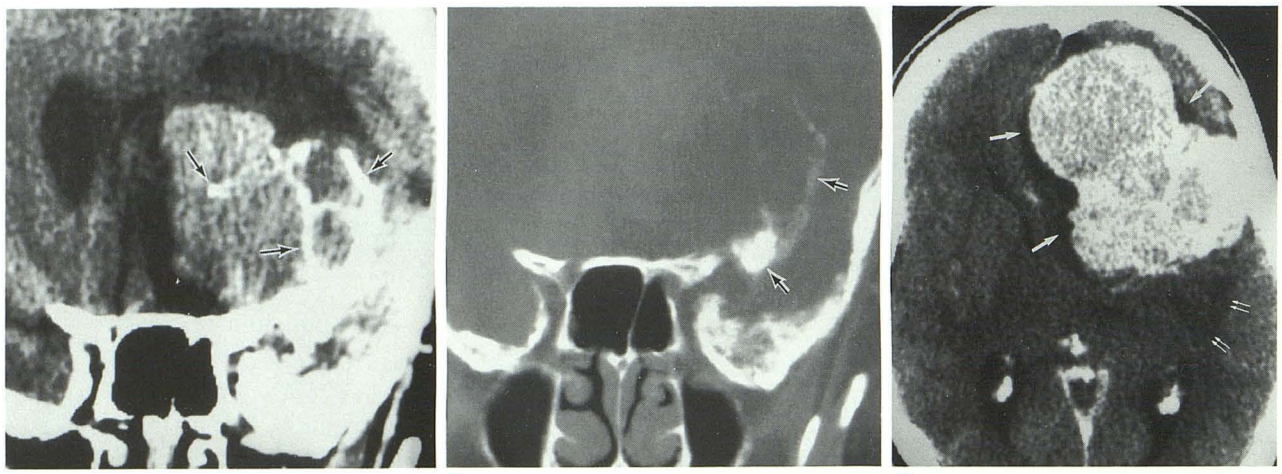

A B C

Fig. 1. *A*, Coronal head CT scan without contrast shows a hyperdense globular mass with focal calcifications (*outlined arrows*) arising from a thickened sphenoid wing.

B, Bone window (same level as in *A*) demonstrates alteration of bony architecture with thickening and hyperostosis of the lesser and greater sphenoid alae. Calcification within the mass is more evident (*outlined arrows*).

C, Postcontrast axial scan shows a homogeneously enhancing well-circumscribed mass with a surrounding low-density rim representing a fluid-filled cleft (*single-white arrows*). Left frontal horn compression and displacement as well as white matter edema (*double white arrows*) are also seen.

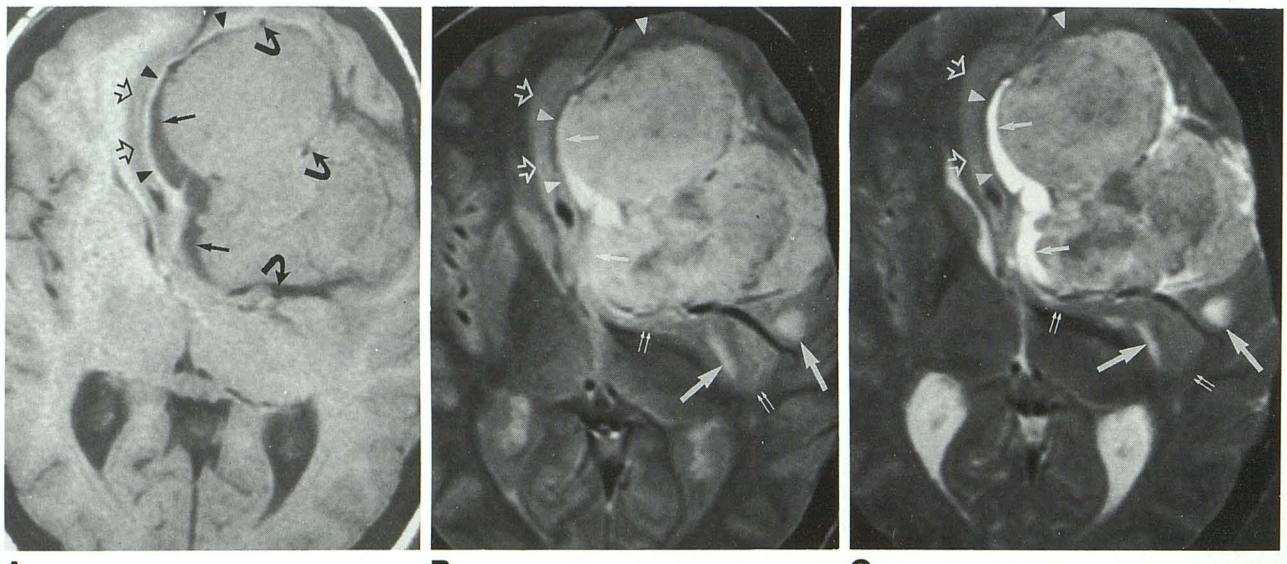

A B C

Fig. 2. *A*, Axial noncontrast T1-weighted MR scan (TR = 600 msec, TE = 20 msec) demonstrates a well-delineated globular left frontal mass that is isointense to gray matter. A low-intensity rim, the CSF cleft (*small single black arrows*), surrounds the mass. A thin, intermediate signal fibrous capsule (*black arrowheads*) is interposed between the fluid-filled cleft and the adjacent displaced cortex (*open black arrows*). Note the presence of punctate and curvilinear flow voids (*curved black arrows*) within (dural vascular supply) and around the mass (pial arterial supply, draining veins).

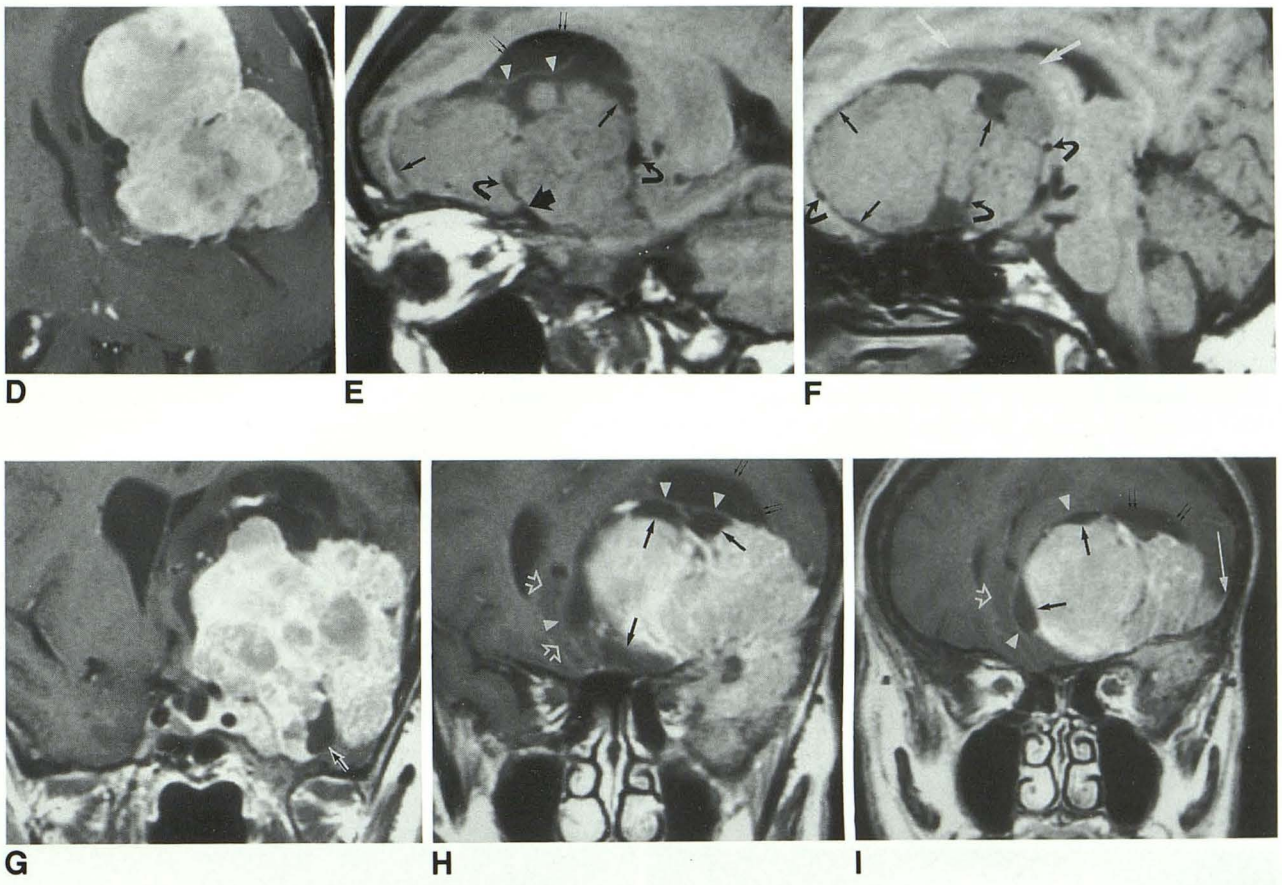

Fig. 2.—*Continued. B*, Axial balanced MR scan (TR = 2800 msec, TE = 30 msec) at the same level as *A* shows the mass is moderately but inhomogeneously hyperintense. The surrounding fluid-filled cleft (*small single white arrows*) is hyperintense compared to cerebrospinal fluid in the lateral ventricles while the fibrous capsule (*white arrowheads*) is relatively hypointense to the displaced gray matter (*open white arrows*). Edema (*double white arrows*) is present in the adjacent white matter. Focal intraparenchymal hyperintensities represent encephalomalacic changes (*large single white arrows*).

C, Axial T2-weighted MR scan (TR = 2800 msec, TE = 80 msec) at the same level as *A* and *B* shows the tumor mass is primarily isointense with cortex. The heterogeneous signal within the mass is more apparent on this sequence. The fluid-filled cleft (*small single white arrows*) surrounding the mass is clearly identified. The fibrous capsule (*white arrowheads*) now appears even more hypointense than on the balanced scan (*B*). The displaced gray-white interface (*open white arrows*) is seen as are focal parenchymal encephalomalacic changes (*large single white arrows*) and minimal white matter edema (*double white arrows*).

D, Postcontrast T1WI shows the mass enhances strongly but inhomogeneously.

Scans (*E–I*) show features of meningiomas. Sagittal T1-weighted (TR = 600 msec, TE = 20 msec) scans without contrast (*E* and *F*) demonstrate the tumor arising from the sphenoid wing (*E*, *wide black arrow* represents the enostotic spur) and extending into both anterior and middle cranial fossae. The fibrous capsule that often separates meningiomas from adjacent brain is also clearly seen (*E*, *white arrowheads*). An underlying fluid "cleft" (*E* and *F*, *small single black arrows*) surrounds the tumor. Note the adjacent intraparenchymal cyst (*E*, *double black arrows*) and encephalomalacia (*F*, *large single white arrows*). Prominent peripheral vessels (pial arterial supply, draining veins) and a central vascular pedicle are indicated by the curved arrows.

G, Coronal postcontrast T1-weighted scan through the cavernous sinus shows tumor invasion with encasement of the internal carotid artery. Note that signal void (*outlined arrow*) corresponding to the calcification seen in Figure 1B. More anterior scans demonstrate the fibrous capsule (*H* and *I*, *white arrowheads*), the fluid-filled cleft (*H* and *I*, *small single black arrows*) surrounding the tumor, and the adjacent intraparenchymal cyst (*H* and *I*,, *double black arrows*). Note the displaced gray-white matter interface (*H* and *I*, *open arrows*). The left lesser and greater sphenoid alae are thickened by the enhancing tumor. A small dural "tail" is seen in *I* (*long white arrow*).

Pathology

Dural Attachment

The tumor in this case has a typical broad dural attachment. Meningiomas can also be pedunculated (with a narrow dural attachment) or flat ("meningioma en plaque") (1, 3). Tumors with no apparent dural attachment may be located in the lateral ventricles, diploic spaces, and even in the paranasal sinuses (3).

Histology

Three types of "classic" meningiomas are generally described: Meningothelial (syncytial), fibroblastic, and transitional (1). Fibroblastic tumors consist of thin, spindle-shaped cells in a dense collagen matrix. Syncytial tumors consist of sheets of contiguous polygonal cells with fibrous trabeculae delineating lobules. Microcystic changes and nuclear vesicles are frequent in this histologic type. Transitional tumors, exemplified by our case, represent a mixture of both fibroblastic and synctial characteristics. Central lobules of polygonal cells surrounded by concentric whorls of elongated cells are seen (Figs. 4A and 4B). This subtype frequently contains psammoma bodies (concentric lamina of calcium salts). A fourth category, angioblastic meningioma, was formerly used to describe what are now recognized as several different types of tumor including highly vascular meningiomas, hemangiopericytomas, and hemangioblastomas (3).

Local Effects

The effects of meningiomas on surrounding brain tissue include mass effect, displacement of the gray-white interface, edema, and peritumoral encephalomalacic changes (Footnote A). The tumor illustrated here compressed the lateral ventricles and caused subfalcine herniation (Figs. 2A-2D, 2G-2I, and 3A-2B).

Edema associated with meningiomas may be either focal (Figs. 1C, 2B, and 2C, double white arrows; Fig. 4C) or holohemispheric (4). Various etiologies have been proposed. The edema may be secondary to compressive ischemia with compromise of the blood-brain barrier, venous mechanical obstruction, elevated hydrostatic pressure within the tumor (secondary to hemorrhage or rich vascularity), or a secretory-excretory phenomenon within

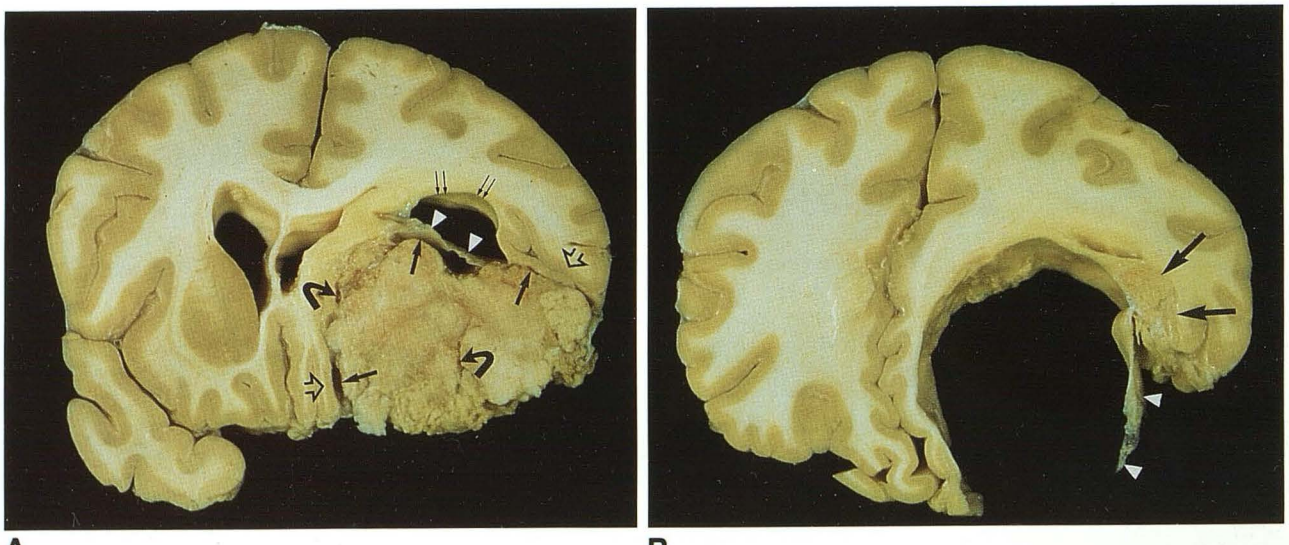

A B

Fig. 3. *A*, Coronal pathologic brain section with tumor in situ demonstrates the surrounding cerebrospinal fluid cleft (*small single black arrows*), fibrous capsule (*white arrowheads*), and intraparenchymal cyst (*double black arrows*). A large vessel in the central vascular pedicle and a prominent surface vessel are indicated by *curved black arrows*. Also note the displaced gray-white interface (*open black arrows*), ventricular compression, and midline shift.

B, Coronal pathologic brain section with tumor removed demonstrates the fibrous capsule (*white arrowheads*), which separated the intraaxial cyst from the CSF cleft surrounding the tumor. (The fibrous capsule on the MR scans is also indicated by *arrowheads*). Encephalomalacic changes (*large single black arrows*) and mass effect are present. This section most closely corresponds to scan in Figure 2I.

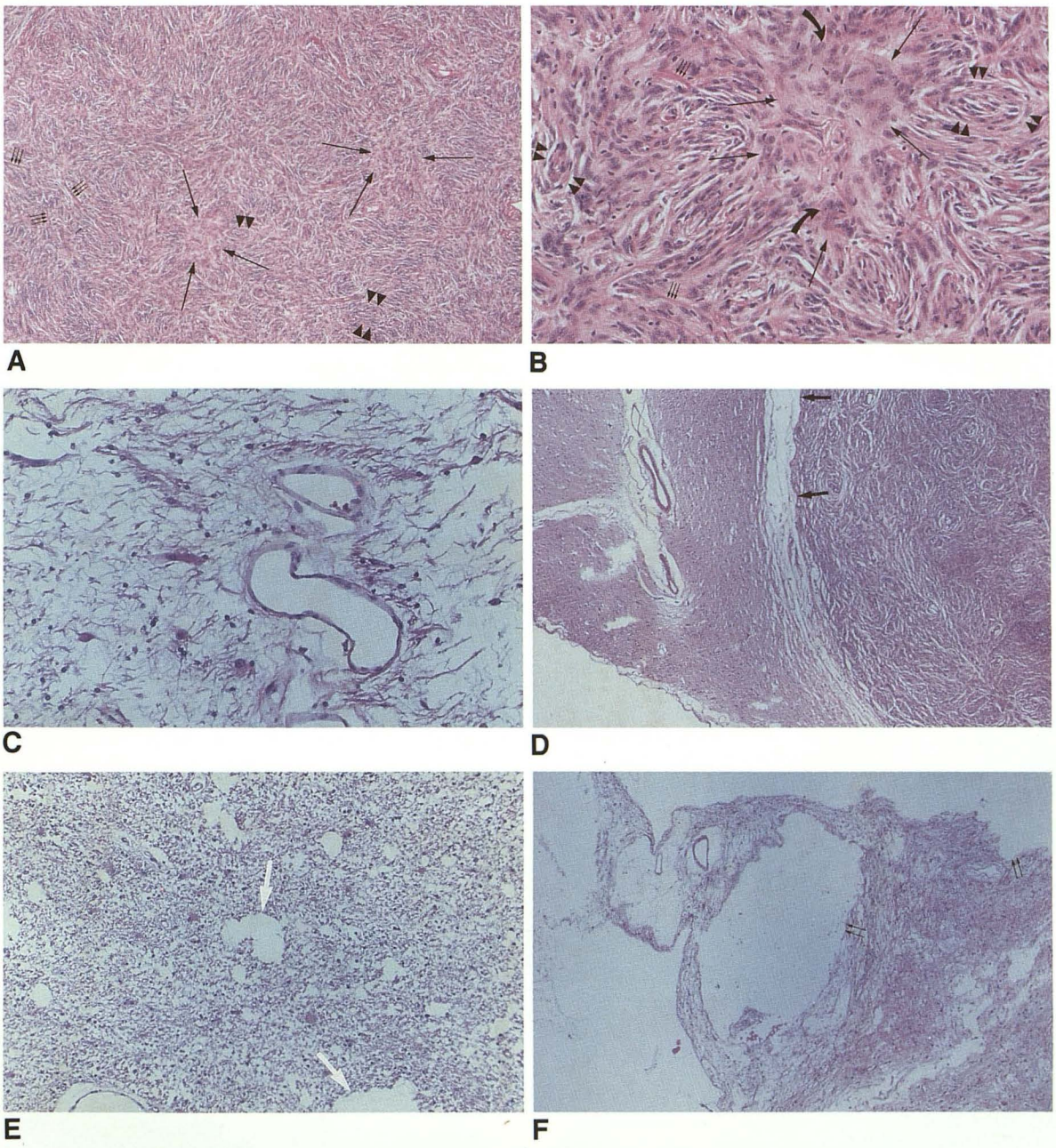

Fig. 4. *A* and *B*, High-power photomicrograph of the tumor, hematoxylin and eosin stain. Lobules of polygonal shaped meningioma cells (*long black arrows*) surrounded by whorls of elongated spindle-shaped meningioma cells (*double arrowheads*) and interdigitating connective tissue (*small triple arrows*) are characteristic of transitional meningioma. Note bland cytologic appearance of the tumor nuclei (*long curved arrows*).

C, High-power photomicrograph of the edematous area seen on MR (Figs. 2B and 2C, double white arrows) shows two small venules and markedly edematous white matter with a few reactive astrocytes.

D, Low-power photomicrograph shows the meningioma (seen on the right) displacing ("buckling") and compressing otherwise normal brain (seen on the left). Note the prominent arachnoid-lined cerebrospinal fluid cleft (*small single arrows*) between the tumor and adjacent brain.

E, High-power photomicrograph (from same area of brain indicated by the large single white arrows in Fig. 2F) shows microcystic encephalomalacic changes (*large white arrows*) and edema with reactive astrocytosis in the brain adjacent to the tumor.

F, Low-power photomicrograph shows confluent areas of cyst formation (*double black arrows*; same as Figs. 2E and 2H) in adjacent brain.

the tumor cells (4). In order for edema to penetrate into the white matter, there must be disruption of the arachnoid and pia mater as well as the cortical gray matter (4). It has been postulated that focal edema results from pressure necrosis while more extensive edema is vasogenic in origin (5).

In contrast to intraaxial neoplasms, meningiomas are extraaxial masses and as such characteristically displace the gray-white matter junction that appears to "buckle" around the growing tumor (Figs. 2A-C, 2H, 2I, and 3A, open arrows; Fig. 4D) (6).

Vascularity

Nearly three-quarters of all meningiomas receive their primary vascular supply from dural vessels. They may also parasitize pial supply from internal carotid artery branches (7, 8). Meningiomas are characteristically supplied by a prominent central vascular pedicle with fan-like radiations of smaller vessels and a more peripheral plexus of pial vessels that supplies the surface (Figs. 2A, 2E-2F, and 3A, curved arrows). There is no blood-brain barrier within the neoplastic tissue and there are open, tortuous gasp junctions between the vascular endothelial cells (9).

Secondary Features

Meningiomas demonstrate both mesenchymal and epithelial characteristics. Mesenchymal differentiation may lead to xanthomatous, lipoblastic, myxoid, chondroblastic, and osteoblastic features. Epithelial differentiation is manifested by papillary formation, desmosomal attachments between cells (these intercellular junctions are characteristic of epithelium) and tumor markers such as carcinoembryonic antigen (10). These tumors may also demonstrate pigmentation with melanin, related to neural crest derivation (1). Calcium in psammoma bodies is a characteristic of transitional meningiomas.

Central necrosis may occur in any type of meningioma whether benign or malignant. Gross intratumoral cystic degeneration and spontaneous hemorrhage are both relatively rare. When present, intratumoral cysts are usually small (Fig. 4E) and peripherally located (Footnote A). Large cysts (Fig. 4F) are secondary to degenerative changes or the confluence of microcysts. Peritumoral cysts, separated from the meningioma by a distinct "capsule", may be lined with arachnoid cells and filled with cerebrospinal fluid (CSF) (Fig. 4D), suggesting blockage of CSF drainage secondary to arachnoid adhesions around the tumor. Cysts within the adjacent brain may also occur (Figs. 2E, 2H, 2I, and 3A, double black arrows). These intraparenchymal cysts are typically lined with glial or connective tissue and may represent an astrocytic reaction to the tumor (11). Frank encephalomalacic changes, probably due to pressure necrosis, can sometimes be seen (Figs. 2B-C, 2F, and 3B, large arrows).

Osseous Changes

A distinguishing feature of meningiomas is the frequent presence of associated osseous changes. These include corticated pressure erosion by the tumor mass, bone destruction, and hyperostosis (Footnote A). The areas most frequently affected are the skull base and anterior half of the calvarial vault. On pathologic specimens, the medullary spaces of bone are often filled with clumps of tumor cells. It has been postulated that the tumor cells directly produce more bone; the osteoblastic activity associated with certain meningiomas would support this theory (1).

The osteolytic changes associated with meningiomas may be related to more rapid tumor

Fig. 5. Coronal pathologic brain section in another case. This sphenoid-wing meningioma underwent sarcomatous degeneration and directly invates the adjacent brain parenchyma. Note loss of an identifiable brain-tumor interface (compare with Figs. 3A and 3B) (From the Rubinstein Collection; Department of Neuropathology, Armed Forces Institute of Pathology, Washington, DC).

growth. Thickening of the inner table of the skull, which has also been noted, has not been associated with tumor invasion but rather is a reactive change. There is a tendency for the dura to detach from the bone, which impairs blood supply through Volkmann's canals and stimulates deposition of subperiosteal bone. A nipple-like boss may be left along the inner table of the skull (1). This enostotic spur or site of focal hyperostosis at the vascular pedicle site is highly suggestive of meningioma (Figs. 2E and 5, wide black arrow). This identifies its point of origin from the dura (Footnote A).

Our case demonstrates both osteoblastic and osteolytic bony changes. The normal architecture of the sphenoid bone has been destroyed and replaced by regions of less organized hyperostosis (Figs. 1B, 2H, and 2I).

Brain-Tumor Interface

Another important feature of meningiomas is the brain-tumor interface. Most meningiomas are easily separable from brain at surgical resection by an intervening connective tissue capsule (12). Our case demonstrates this find-

TABLE 1: Common features of meningiomas

Age	Peak in fifth and sixth decades
Gender	Female predilection
Location	Supratentorial, convexity, basisphenoid; abutting a dural surface
Density on CT	Hyperdense
Intensity on MR	Isointense to gray matter on T1 and T2WI
Enhancement	
1. Postcontrast CT	Homogeneous intense enhancement.
2. Postcontrast MR	Intense enhancement, often more heterogeneous than on CT; adjacent dural enhancement common
Osseous changes	Bone destruction, hyperostosis
Local effects on surrounding brain	Peritumoral edema, displaced gray-white interface, mass effect, encephalomalacia
Secondary features	Calcified psammoma bodies; xanthomatous, lipoblastic, myxoid, chondroblastic, or osteoblastic changes
Brain-tumor interface	CSF cleft, vascular or connective tissue capsule
Vascular supply	Dural vessels supply center; pial vessels supply periphery
Histology	Meningothelial (syncytial), transitional, fibroblastic

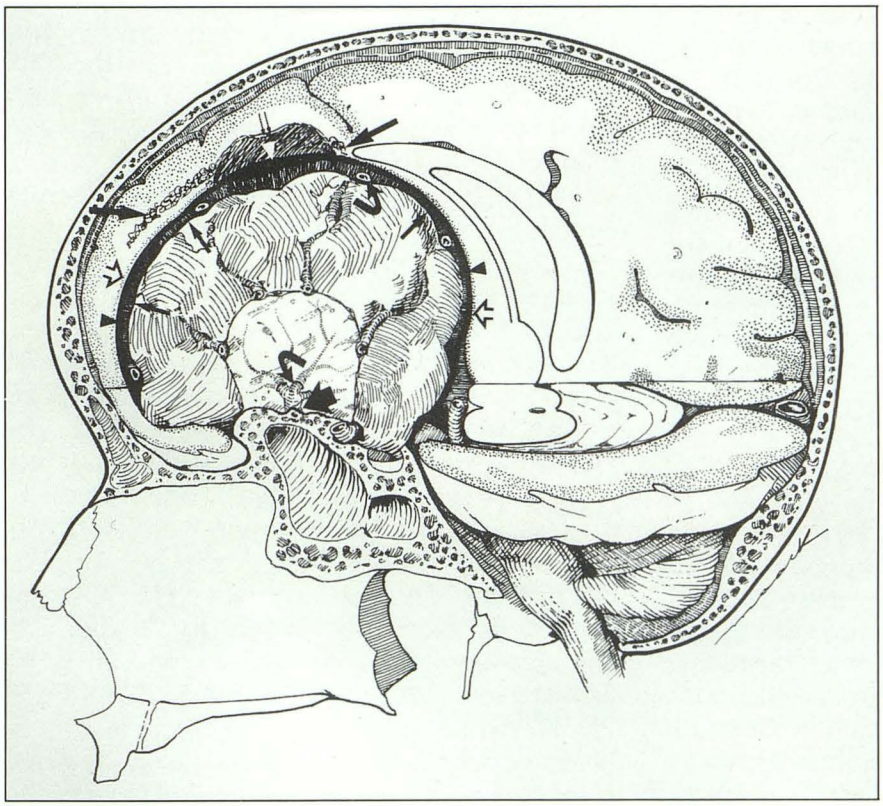

Fig. 6. Anatomic diagram summarizes the pathologic findings in a typical basisphenoid meningioma. The lobular tumor extends into the anterior and middle cranial fossae, invading the cavernous sinus and encasing the supraclinoid carotid artery. Fluid-filled cleft = *small single arrows*; fibrous capsule = *arrowheads*; displaced cortex = *open arrows*; parenchymal encephalomalacic changes = *single large arrows*; focal intraparenchymal cyst = *double arrows*; vessels = *curved arrows* (both the central vascular pedicle and peripheral pial vessels—arteries and draining veins—are shown). Sphenoid hyperostosis with an enostotic spur (*wide black arrow*) is also depicted.

ing (Fig. 3, arrowheads). Meningiomas are often surrounded by a pool of CSF in an area of focal pressure atrophy, possibly due to local obstruction of normal drainage. A fibrous or venous vascular capsule (Figs. 3A, 3B, and 6, arrowheads) may also be present overlying the CSF "cleft" (13).

Imaging

Computed Tomography

Meningiomas generally appear as well-circumscribed lobular lesions. Most have homogeneous high density on nonenhanced CT scans, 25 to 33% are isodense, approximately 1% are hypodense, and some cases demonstrate mixed attenuation. CT detects calcification in 15%–20%. Most meningiomas demonstrate moderate to intense enhancement following contrast administration (Footnote A). The degree of enhancement is dependent both on tumor vascularity and extracellular accumulation of contrast (9). This case is hyperdense on nonenhanced CT scans (Fig. 1A) with focal areas of calcification (Figs. 1A-1B, outlined arrows) and enhances on postcontrast examination (Fig. 1C).

Peritumoral edema is seen in 60% of meningiomas (14). In our case, minimal edema is present and is seen as low density within the white matter adjacent to the tumor (Fig. 1C, double white arrows); occasionally edema may spread throughout the hemispheric white matter.

Associated bony changes are seen in approximately 15%–20% of meningiomas (Footnote A). Our case demonstrates destruction of the lesser and greater sphenoid alae that have been replaced with regions of less organized hyperostosis (Fig. 1B).

MR Imaging

Meningiomas typically appear isointense with gray matter on both T1- and T2-weighted images and enhance intensely with contrast (Figs. 2A- 2D) (13). While imaging studies can not reliably predict meningioma histology, those with a high proportion of calcifications and fibrous changes most likely demonstrate lower signal intensities on T2WI than do highly cellular or vascular meningiomas (15).

Intratumoral inhomogeneities are often seen on MR imaging (Figs. 2B–2D). Calcifications usually appear as focal areas of hypointensity on T1- and T2-weighted MR images (Fig. 2G, outlined arrow). Other causes of low signal intensity on T1WI include central necrosis, pseudocysts, vascular spaces, and infrequently, cystic degeneration and bony metaplasia (16, 17). Spontaneous intratumoral hemorrhage is uncommon; it occurs more frequently in the highly vascular meningiomas (1). Xanthomatous, lipoblastic, myxoid, chondroblastic, and osteoblastic changes can also account for focal signal heterogeneities (Footnote A).

Certain pathologic features are better reflected on MR images than on CT. The displaced gray-white interface is more clearly demonstrated (Figs. 2A-2D, 2H, and 2I, open arrows). Peritumoral edema appears as a hypointense region on T1-weighted images and a hyperintense region on T2WI that surrounds the tumor and extends into the white matter tracts (Figs. 2B and 2C, double white arrows). Adjacent encephalomalacic changes are also clearly seen (Figs. 2B, 2C, and 2F, large single white arrows).

Multiplanar MR imaging demonstrates origin of the tumor from the sphenoid ridge on coronal and sagittal images (Figs. 2E and 2H). Invasion of the cavernous sinus with encasement of the supraclinoid carotid artery is easily identified (Fig. 2G).

Meningiomas are generally well-circumscribed with a surrounding low-intensity rim on MR images. This particular tumor is surrounded by a CSF cleft, seen in the pathologic specimen (Fig. 3A, small single black arrows), that appears as a low-intensity rim on T1WI (Figs. 2A, 2E-2F, and 2H-2I, small single black arrows) and is hyperintense on T2WI (Figs. 2B-2C, small single white arrows). The punctate regions of signal void within the low-intensity rim most likely represent marginal blood vessels seen in cross section (Figs. 2A, 2E, 2F, and 3A curved black arrows). The adjacent slightly hyperintense rim on T1WI (Fig. 2A, black arrowheads; Figs. 2E, 2H, and 2I, white arrowheads) that is hypointense on T2WI (Figs. 2B-2C, white arrowheads) represents the fibrous connective tissue capsule (Fig. 3, white arrowheads) that separates the tumor from the

overlying intraparenchymal cyst (Figs. 2E, 2H, 2I, and 3A, double black arrows). Most meningiomas have a characteristic surrounding low-intensity rim on T1-weighted MR images that is indicative of a CSF cleft, a venous capsule, or a combination of both (13). However, some meningiomas do invade the brain parenchyma (Fig. 5) and may thus lose this characteristic MR finding (18).

The associated osseous changes are less well-defined with MR than with CT. Regions where the bony cortex is infiltrated and medullary spaces are filled with clumps of tumor cells may be seen on MR as abnormally increased intensity of the bony cortex that blends in with the normal high intensity of the diploic spaces. The normal cortical-medullary interface becomes obliterated resulting in an amorphous appearance of the affected bone (Figs. 2H, and 2I) (19).

A feature that is suggestive of, though not specific for, meningiomas is adjacent dural enhancement in the form of a "dural tail." Dural thickening around meningiomas has been noted in up to 60% of cases (20). In our case, the tumor shows some faint adjacent dural enhancement (Fig. 2I, long white arrow). While thickened dura may occasionally represent actual tumor invasion (21), nonneoplastic reactive changes consisting of loose connective tissue proliferation, hypervascularity, and vascular dilatation are common (22).

Summary

This case shows many of the imaging features classically associated with meningiomas. The illustrations show common location, shape, and local effects as well as enhancement characteristics. Hyperostosis and bone destruction, a fluid "cleft" surrounding the extraaxial mass, gray-white interface displacement, and secondary intraparenchymal changes are correlated with gross pathology findings. These key features are summarized in Table 1 and the composite anatomic diagram (Fig. 6).

References

1. Russell DS, Rubenstein LJ. *Pathology of tumours of the nervous system. 5th ed.* London: Edward Arnold, 1989:449–469
2. Kepes, JJ. Presidential Address. The histopathology of meningiomas: a reflection of origins and expected behavior? *J Neuropathol Exp Neurol* 1986;45:95–107
3. Okazaki H. *Fundamentals of neuropathology: morphologic basis of neurologic disorders. 2nd ed.* New York: Igaku-Shoin, 1989:237–244
4. Go GK, Wilmink JT, Molenaar WM. Peritumoral brain edema associated with meningiomas. *Neurosurgery* 1988;23:175–179
5. Trittmacher S, Traupe H, Schmid A. Pre- and postoperative changes in brain tissue surrounding a meningioma. *Neurosurgery* 1988;22:882–885.
6. George AE, Russell EJ, Kricheff IT. White matter buckling: CT sign of extraaxial intracranial mass. *AJNR* 1980;1:425–430
7. Servo A, Porras M, Jaaskelainen J, Paetau A, Haltia M. Computed tomography and angiography do not reliably discriminate malignant meningiomas from benign ones. *Neuroradiology* 1990;32:94–97
8. Siegelman ES, Mishkin MM, Taveras JM. Past, present, and future of radiology of meningioma (radiologic history exhibit). *Radiographics* 1991;11:899–910
9. Watabe T, Azume T. T1 and T2 measurements of meningiomas and neuromas before and after Gd-DTPA. *AJNR* 1989;10:463–470
10. Rohringer M, Sutherland G, Louw DF, Sima AAF. Incidence and clinicopathologic features of meningioma. *J Neurosurg* 1989;71:665–672
11. Maiuri F, Benvenuti D, DeSimon MR, Cirillo S, Corriero G, Giamundo A. Cystic lesions associated with meningiomas. *Surg Neurol* 1986;26:591–597
12. Nakasu S, Hirano A, Llena JF, Shimura T, Handa J. Interface between the meningioma and the brain. *Surg Neurol* 1989;32:206–212
13. Spagnoli MV, Goldberg HI, Grossman RI, et al. Intracranial meningiomas: high-field MR imaging. *Radiology* 1986;161:369–375
14. Bradac GB, Fertszt R, Bender A, Schorner W. Peritumoral edema in meningiomas: a radiological and histological study. *Neuroradiology* 1986;28:304–312.
15. Elster AD, Venkata RC, Tucker HG, Richardson DN, Contento JC. Meningiomas: MR and histopathologic features. *Radiology* 1989;170:857–862
16. Demaerel P, Wilms G, Lammens M, et al. Intracranial meningiomas: correlation between MR imaging and histology in fifty patients. *J Comput Assist Tomogr* 1991;15:45–51
17. Buetow MP, Buetow PC, Smirniotopoulos JG. Typical, atypical, and misleading features in meningioma. *Radiographics* 1991 (in press)
18. Nakasu S, Nakasu Y, Matsumura K, Matsuda M, Handa J. Interface between the meningioma and the brain on magnetic resonance imaging. *Surg Neurol* 1990;33:105–116
19. Zimmerman RD, Fleming CA, Saint-Louis LA, Lee BCP, Manning JJ, Deck MDF. Magnetic resonance imaging of meningiomas. *AJNR* 1985;6:149–157
20. Goldsher D, Litt AW, Pinto RS, Bannon KR, Kricheff II. Dural "tail" associated with meningiomas on Gd-DTPA-enhanced MR images: characteristics, differential diagnostic value, and possible implications for treatment. *Radiology* 1990;176:447–450
21. Wilms G, Lammens M, Marchal G, et al. Prominent dural enhancement adjacent to nonmeningiomatous malignant lesions on contrast-enhanced MR images. *AJNR* 1991;12:761–764
22. Tokumaru A, O'uchi T, Eguchi T, et al. Prominent meningeal enhancement adjacent to meningioma on Gd-DTPA-enhanced MR images: histopathologic correlation. *Radiology* 1990;175:431–433